A method for measurement of human asparagine synthetase (ASNS) activity and application to ASNS protein variants associated with ASNS deficiency

Mario C. Chang [ID] [1,*,†], Stephen J. Staklinski [ID] [1,2,†], Matthew E. Merritt [ID] [1] Michael S. Kilberg[1]

[1]Department of Biochemistry and Molecular Biology, University of Florida College of Medicine, Gainesville, FL 32610, United States
[2]School of Biological Sciences, Cold Spring Harbor Laboratory, Cold Spring Harbor, NY 11724, United States

*Correspondence address. Department of Biochemistry and Molecular Biology, University of Florida College of Medicine, 1200 Newell Drive, Box 100245, Gainesville, FL 32610, United States. E-mail: marioc14@ufl.edu

[†]Equally contributed authors.

Abstract

Human asparagine synthetase (ASNS) catalyzes the conversion of aspartate to asparagine in an ATP-dependent reaction that utilizes glutamine as a nitrogen source while generating glutamate, AMP, and pyrophosphate as additional products. Asparagine Synthetase Deficiency (ASNSD) is an inborn error of metabolism in which children present with homozygous or compound heterozygous mutations in the *ASNS* gene. These mutations result in ASNS variant protein expression. It is believed that these variant ASNS proteins have reduced enzymatic activity or stability resulting in a lack of sufficient asparagine production for cell function. Reduced asparagine production by ASNS appears to severely hinder fetal brain development. Although a variety of approaches for assaying ASNS activity have been reported, we present here a straightforward method for the *in vitro* enzymatic analysis by detection of AMP production. Our method overcomes limitations in technical feasibility, signal detection, and reproducibility experienced by prior methods like high-performance liquid chromatography, ninhydrin staining, and radioactive tracing. After purification of FLAG-tagged R49Q, G289A, and T337I ASNS variants from stably expressing HEK 293T cells, this method revealed a reduction in activity of 90, 36, and 96%, respectively. Thus, ASNS protein expression and purification, followed by enzymatic activity analysis, has provided a relatively simple protocol to evaluate structure–function relationships for ASNS variants reported for ASNSD patients.

Graphical Abstract
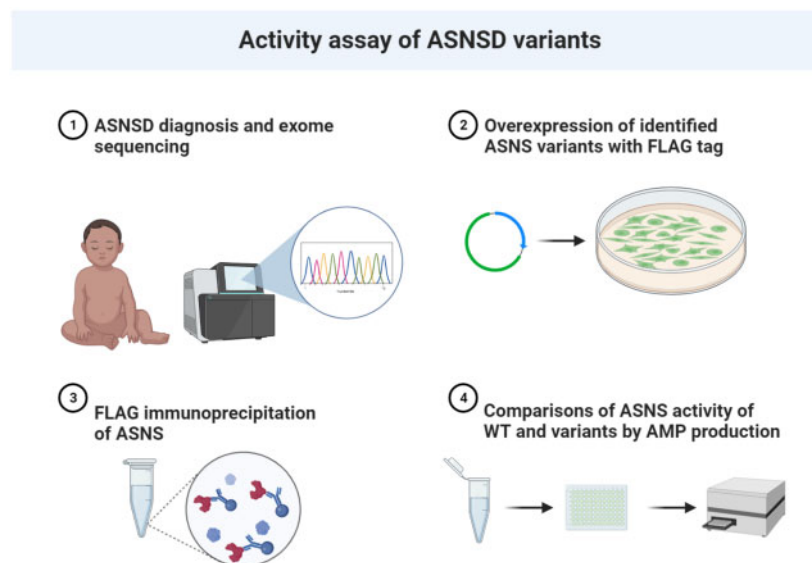
Keywords: metabolism; amino acids; asparagine; pediatrics; neurotransmitters; enzyme deficiency; enzyme assay

Introduction

Human asparagine synthetase (ASNS) is a cytoplasmic enzyme that catalyzes the conversion of aspartate to asparagine (Asn) in an ATP-dependent reaction that utilizes glutamine as a nitrogen source, while also generating glutamate, AMP, and pyrophosphate (PPi) [1]. Based on whole animal growth studies, Asn is considered a "non-essential" dietary amino acid, but for a given cell, an ASNS enzyme deficiency that is sufficiently large leads to extracellular Asn dependence. It is the only human enzyme that synthesizes Asn, making it a metabolic vulnerability for which mutations can lead to disease. Asn metabolism and the impact of ASNS activity have received considerable attention in cancer, beginning with the observation that childhood acute lymphoblastic leukemia (ALL) is susceptible to treatment with bacterial asparaginase (ASNase). Primary ALL cells and many ALL-derived cell lines exhibit little or no detectable ASNS activity and therefore, their growth is prevented by extracellular Asn depletion [2–7]. Consequently, a standard component of combination chemotherapy for childhood ALL is the rapid depletion of plasma Asn by infusion of bacterial ASNase [8, 9]. Additionally, ASNS has been reported to serve as a robust promoter of tumor growth and metastatic disease over a range of different cancers [10]. Aberrantly increased ASNS protein expression promotes tumor proliferation by protecting cell cycle regulation, evading ASNase sensitivity, and generating Asn to allow for unhampered protein synthesis, amino acid exchange across the plasma membrane, and coupling cell proliferation to mitochondrial respiration [10–12].

In 2013, biallelic mutations of the *ASNS* gene (NM_133436.3) were reported as the cause of asparagine synthetase deficiency (ASNSD), a rare congenital neurological disorder [13]. Children with ASNSD often present within the first year of life with congenital microcephaly, early onset seizures, axial hypotonia, severe appendicular spasticity, and in severe cases, continued brain atrophy and mortality at a premature age [13–16]. The biochemical mechanisms that cause the overt ASNSD symptoms are not well understood. Although ASNSD is associated with defects in peripheral organs, there is a prominent deleterious effect on brain structure and function. The three nitrogen-rich amino acids, Asn, glutamine, and histidine, are transported across the luminal surface of the endothelial cells that comprise the blood–brain barrier by a facilitated transporter activity [17]. Given that this transporter has an equilibrating, bidirectional activity, Asn is not actively accumulated within the brain. To further prevent excess nitrogen accumulation within the brain, on the abluminal membrane of the endothelial layer, a Na^+-dependent transporter catalyzes the efflux of Asn from the brain toward the circulation. Thus, brain tissue relies heavily on localized production of Asn through ASNS enzymatic activity. This cooperative arrangement protects the brain from excess nitrogen but also explains why a genetically derived decrease in brain ASNS catalytic activity leads to the severe reduction of brain development observed in ASNSD patients.

Currently, patients suspected of having ASNSD can only be diagnosed through expensive and time-consuming whole exome DNA sequencing, making rapid and routine screening of newborns impossible. One might consider changes in plasma or cerebral spinal fluid Asn levels as a screening mechanism, but neither is predictably altered in ASNSD patients. Circulating plasma Asn was reduced in only half of the ASNSD patients tested, reviewed in Gupta et al. (2017), and cerebral spinal fluid Asn content was below detection limits in only about half of

ASNSD patients tested [18–21]. Nonetheless, a straightforward means of assessing ASNS enzymatic activity could serve as an additional diagnostic screen for ASNSD. A number of methods like ninhydrin staining, HPLC, and radioactive tracing have been developed for assaying ASNS activity [22–24], but they are limited by reproducibility, signal specificity and sensitivity, and technical expertise. Thus, there is a need for a highly reproducible and sensitive ASNS enzyme activity assay. Furthermore, such an assay would also be useful to monitor ASNS activity in newly diagnosed ALL patients as well as those undergoing ASNase therapy, given the potential for the development of ASNase resistance due to increased ASNS expression [10, 14, 25].

Here we present methodology for the purification of active wild-type (WT) and ASNS variant (FLAG-tagged) proteins from human cell extracts and a new approach to assay ASNS activity through the measurement of AMP production (Fig. 1A and B). To illustrate the robustness of the assay, we used an immunoprecipitation-based purification scheme to isolate ASNS protein following ectopic expression of FLAG-tagged ASNS in HEK 293T cells. We document that a luminescence-based AMP assay of ASNS activity provides the basis for a simple and reproducible protocol. The applicability of the assay was shown by measuring the differences in enzyme activity of several ASNS variants that we have previously described for ASNSD patients [26–30].

Materials and methods
Generation of HEK 293T cells that stably express FLAG-tagged ASNS protein

HEK 293T cells (ATCC CRL-3216) were cultured in high glucose Dulbecco's Modified Eagle's Medium (DMEM) (Corning 10-013-CV) supplemented with 10% fetal bovine serum (Bio-Techne S11550), ABAM (streptomycin, penicillin G, and amphotericin B), 1× non-essential amino acids, and 2 mM glutamine. Cells were maintained at 37°C with 5% CO_2 and were plated at 30%–40% confluence, passaged once they achieved 80% confluence, and collected for experiments at about 70%–75% confluence.

A WT ASNS expression plasmid was obtained from Sino Biological (HG16454-CF) and contains a C-terminal linker and FLAG-tag sequence following the ASNS open reading frame. The ASNS sequence was mutated by Q5 site-directed mutagenesis (NEB E0554S) to generate independent plasmids encoding R49Q, G289A, and T337I ASNS variants. The plasmids were purified with the PureYield™ Plasmid Miniprep System (Promega A1223), and the coding regions were confirmed by DNA sequencing. WT and variant ASNS plasmids were transfected into HEK 293T cells with X-tremeGENE 9 transfection reagent (Roche 06 365 787 001) per the manufacturer's protocol and at 48 h post-transfection, the medium was replaced with fresh DMEM. ASNS-expressing stable cell lines for WT and each variant were selected with 100 µg/ml hygromycin B (EMD Millipore 400052-5ML) for 14 days. Cell stocks were suspended in complete DMEM with 10% DMSO and stored in liquid nitrogen. During routine culture, the cells were maintained in 50 µg/ml of hygromycin B.

To confirm ASNS-FLAG expression for each cell line, cell lysates were quantified by a Bradford assay (Bio-Rad 5000006) and subjected to immunoblotting. Cells were lysed in 50 mM Tris, 150 mM NaCl, and 0.1% Triton X-100 and a 30 µg aliquot was loaded per lane on a 4%–15% Mini Criterion TGX gel (Bio-Rad 4561086). Gels were run at a constant current of 0.05 A and transferred onto a polyvinylidene difluoride (PVDF) membrane (Bio-Rad 1620177) at 4°C at 50 V for 1 h. The membrane was blocked for 2 h in 5% non-fat dry milk in TBS-T (30 mM Tris (pH 7.6),
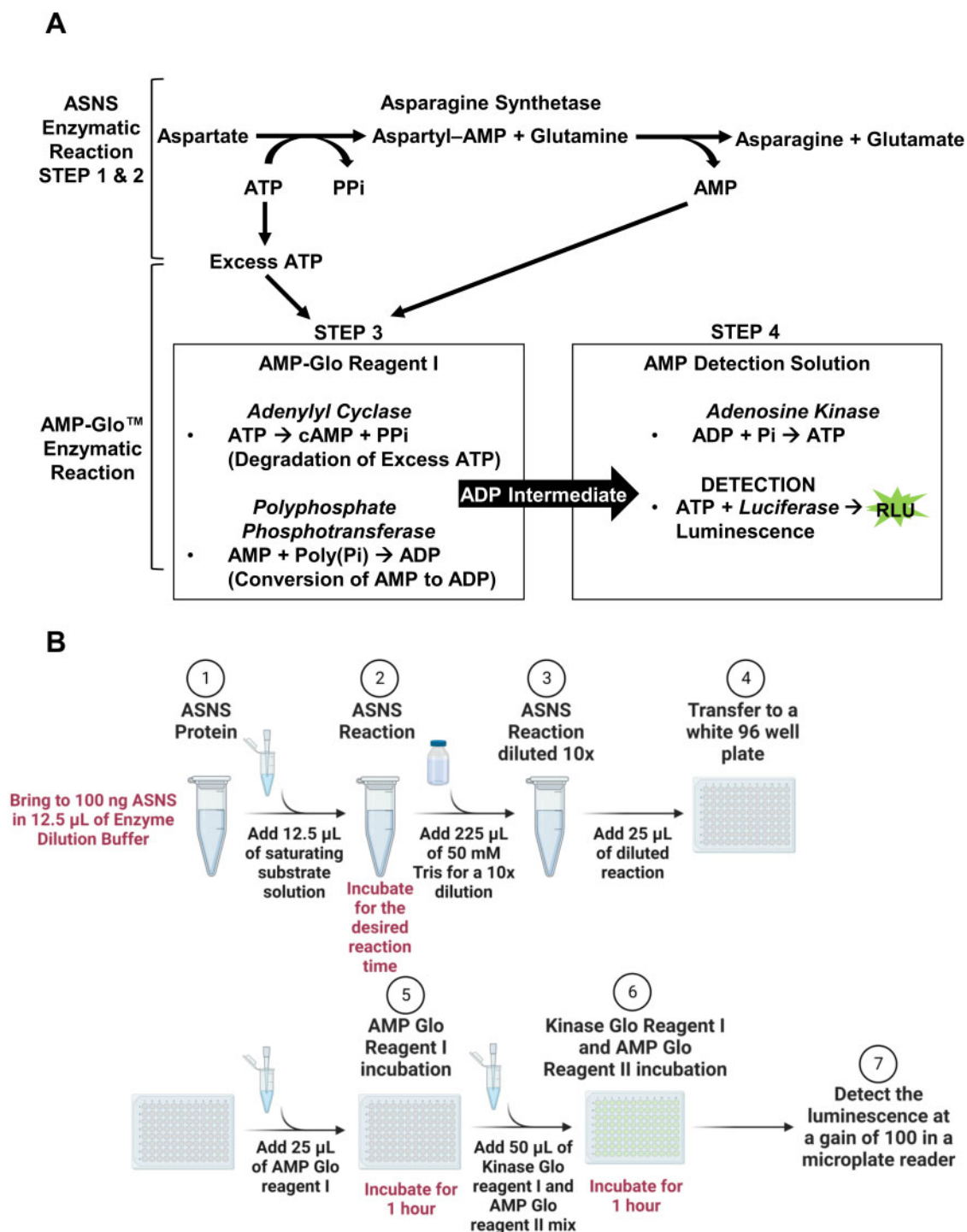
A

B

Figure 1. Flow diagram of ASNS activity assay by AMP detection. (**A**) The ASNS enzymatic reaction is shown (top) and the relationship to the AMP-Glo™ enzymatic reaction kit is indicated below the reaction. Details about each AMP-Glo™ reaction step are provided in the boxes and have been modified as described in the text. (**B**) Schematic depiction of the ASNS AMP-Glo™ activity assay using purified ASNS protein.

200 mM NaCl, and 0.1% Tween-20). Primary anti-FLAG monoclonal antibody (Cell Signaling 14793S) was diluted 1:1000 in TBS-T with 5% non-fat dry milk and added to the blot for 18 h at 4°C. After incubation, the membrane was washed 5 times for 5 min each in TBS-T, and then secondary anti-rabbit HRP antibody (Bio-Rad 170-6515) was diluted 1:5000 and added for 1 h at room temperature. The membrane was washed again, incubated with Pierce™ ECL Western Blotting Substrate (Thermo Scientific 32106), and exposed to Classic autoradiography film (Midwest

Scientific BX57). For GAPDH detection, a 1:8000 dilution of GAPDH monoclonal antibody (Santa Cruz Biotechnology sc-32233) was added to the membrane for 1 h at room temperature. The secondary used was a 1:5000 dilution of anti-mouse HRP antibody (Bio-Rad 170-6516) incubated for 1 h at room temperature.

ASNS protein purification

ASNS-expressing HEK 293T cell lines were grown to near confluency in a 150 mm dish and lysed in 1 ml of 50 mM Tris–HCl, pH

7.5, 150 mM NaCl, and 0.1% Triton X-100 for 15 min on ice followed by centrifugation at 13,000g for 10 min to retain the supernatant. ANTI-FLAG® M2 Affinity Gel (Sigma-Aldrich #F2426) was prepared by washing the gel according to the manufacturer's protocol. An aliquot of 20 µl of packed gel was then incubated with 1 ml of HEK 293T lysate for 18 h at 4°C. The supernatant was removed and the ASNS-FLAG bound gel was washed 3 times with Tris-buffered saline (TBS, 30 mM Tris-HCl, pH 7.6, 200 mM NaCl). FLAG peptide, at a concentration of 150 ng/µl in 100 µl TBS, was added to the gel for 1 h at 4°C to elute the ASNS-FLAG protein by competitive binding. The supernatant containing the purified ASNS protein was recovered and 20% glycerol was added to stabilize the protein for storage. To assess the quality of the purified ASNS-FLAG, a 2 µg aliquot of protein in 1× Laemmli buffer (Bio-Rad 161-0747) was boiled for 5 min and then separated on a 4%–15% Mini Criterion TGX Gel (Bio-Rad 4561083). The gel was stained in 3 g/l of Coomassie R-250 Brilliant Blue (Bio-Rad 161-0400) in 50% methanol, 40% ddH$_2$O, and 10% acetic acid for 18 h. The gel was de-stained in 50% methanol, 40% ddH$_2$O, and 10% acetic acid until the background was nearly clear. The gel was rehydrated in ddH$_2$O for about 5 min and imaged.

As a positive control, enzymatically active WT human ASNS protein (Cys2-Ala561 with a C-terminal HIS tag) was purchased from Novus Biologicals (AS-10193). The original 0.5 mg/ml stock solution from Novus was diluted in sterile storage buffer [25 mM Tris-HCl (pH 8.0), 200 mM NaCl, 0.5 mM TCEP-HCl and 20% (v/v) glycerol] to generate 0.1 mg/ml aliquots of purified protein. Our purified ASNS-FLAG protein and the purchased ASNS-HIS protein aliquots were flash-frozen in liquid nitrogen and stored at −80°C prior to analysis. The amount of purified ASNS protein was quantified by a Bradford assay.

Assay of ASNS activity by AMP production

The enzymatic activity of WT and variant ASNS proteins was assessed by measuring the production of AMP with a commercially available luminescence assay kit (V5011, Promega), and the workflow is detailed in Fig. 1A and B. Assay preparation involved thawing an aliquot of 0.1 mg/ml ASNS protein and an aliquot of AMP-Glo™ I solution on ice. ASNS protein was then diluted to 8 ng/µl (0.1 µg of ASNS per reaction) with enzyme buffer. Enzyme reactions were prepared in triplicate by pipetting 12.5 µl of diluted ASNS or blank buffer samples into 1.5 ml microcentrifuge tubes. The reactions were initiated by adding 12.5 µl of substrate solution, which resulted in a final concentration of 50 mM Tris-HCl (pH 8.0), 10 mM MgCl$_2$, 0.75 mM DTT, 0.05 mg/ml BSA, 10 mM aspartate, 10 mM glutamine, and 1 mM ATP. The reaction was then incubated at room temperature (25°C) for the desired time, after which 225 µl of 50 mM Tris-HCl (pH 7.5) were immediately added to each reaction for a 1:10 dilution to bring AMP levels into a measurable range for the kit. The reaction was incubated for 30 min at room temperature and then diluted 1:10 with 50 mM Tris-HCl, pH 7.5. From each ASNS reaction mixture, three individual 25 µl aliquots were transferred into individual wells of a white-colored 96-well plate suitable for luminescence measurements. The ASNS reaction was quenched by adding 25 µl of AMP-Glo© I solution to each well containing the 25 µl of reaction mixture. The 96-well plate was promptly covered with parafilm and centrifuged at 2000g for 3 min. The plate was then incubated at room temperature for 1 h, after which, 50 µl of AMP detection solution (AMP-Glo© Reagent II + Kinase Glo® One Solution), was pipetted into each well. The plate was immediately sealed with parafilm and centrifuged at 2000g for 3 min. The reactions were then incubated for another 1 h at room temperature. Using a

microplate reader with the gain set to 100, the luminescence of each well was determined as relative luminescent units (Fig. 1B). The nanogram quantities of AMP produced were ascertained by referencing an AMP standard curve covering 0 ng (0 µM) to 86.8 ng (10 µM) AMP. The typical analysis of the standard curve yielded an $R^2 > 0.99$. Luminescent detection was performed using a Synergy 2 Multi-Mode Microplate Reader (7131000, BioTek® Instruments).

Protein modeling

The human ASNS crystal structure (PDB: 6GQ3; Uniprot ID: P08243) was overlaid with that of *Escherichia coli* asparagine synthetase B (PDB: 1CT9) to confirm the similarity in structure and allow for human ASNS modeling in the C-terminal active site based on the location of AMP in the *E. coli* asparagine synthetase B crystal [31]. Within the human protein, variant residues of interest were located utilizing the sequence tool, and the depicted color was changed to highlight each location relative to the whole protein. All modeling was performed with UCSF Chimera software (version 1.15). All other graphic images were created with BioRender.com.

Statistical analysis

All experiments were performed in triplicate to assess variability and repeated at least two separate times with independent samples of protein to document reproducibility. Statistical analysis was performed in Excel using the two-tailed, unpaired homoscedastic Student's *t*-test.

Results

Optimization and validation: measurement of ASNS activity by AMP detection

ASNS assay conditions were optimized using commercially available, purified, and active ASNS enzyme. The reaction time course, ASNS protein concentration, and substrate concentrations were individually analyzed. Time course analysis established that the ASNS reaction was linear over the 10–30 min reaction time tested (Fig. 2A). Using a 30 min reaction time, an ASNS protein concentration curve was assessed at 0.05, 0.1, 0.2, and 0.3 µg protein. The ASNS concentration of 8 ng/µl (0.1 µg) per reaction was determined to be optimal for kinetic measurements (Fig. 2B). Substrate analysis identified that concentrations of 10 mM aspartate, 10 mM glutamine, and 1 mM ATP were sufficient to allow for steady-state kinetics (Fig. 2C and D). From these kinetic analyses, the approximate K_m of aspartate was determined to be 0.53 mM and that for glutamate was 2.4 mM. These values are comparable to the reported 0.38 mM aspartate and 1.90 mM glutamine K_m values previously reported [32], indicating the reliability of this approach for assay of ASNS activity. Once the assay variables were optimized, the purified ASNS protein was used to document that the enzymatic activity of protein-deficient samples (a blank), heat-denatured ASNS protein, and empty samples were minimal. These controls were routinely used in future studies.

Purification of WT and ASNS variant proteins

To illustrate the application of the ASNS assay, ectopic expression and purification of FLAG-tagged WT ASNS protein and ASNS variants associated with previously characterized cases of ASNSD was achieved (Fig. 3). Stable expression was established in HEK 293T cells, and proteins were purified using a FLAG gel immunoprecipitation protocol. Typically, the purified proteins
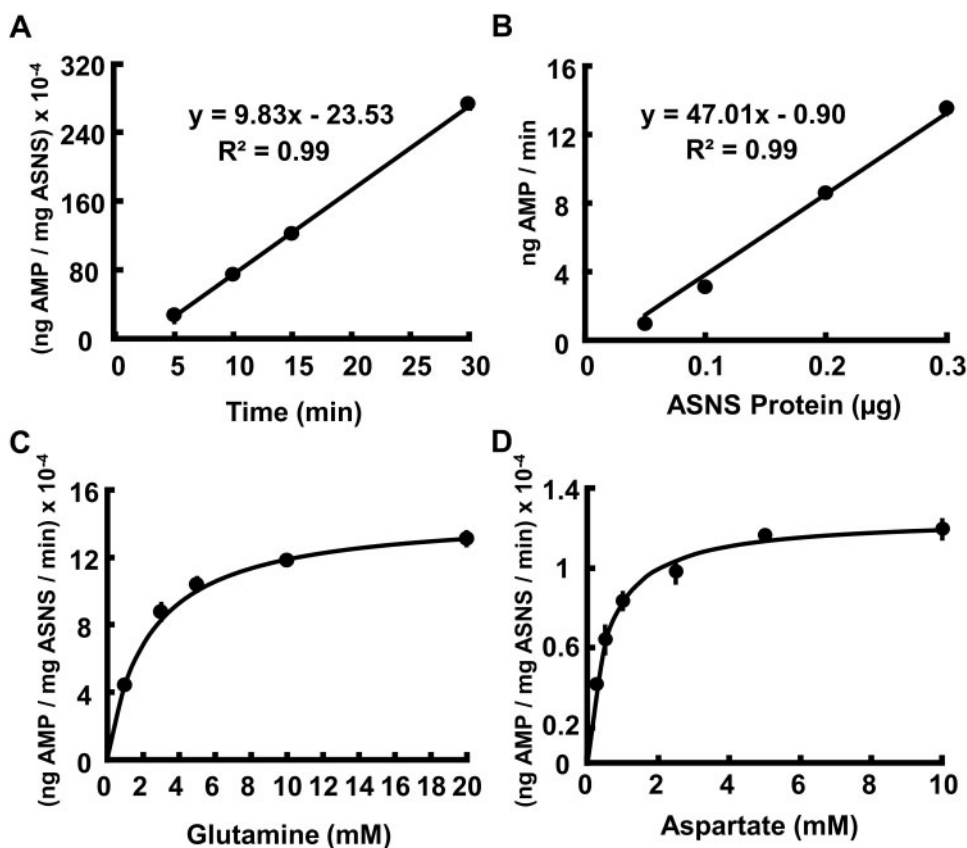
Figure 2. Kinetic analysis of ASNS activity. (**A**) Time course of ASNS activity at 5, 10, 15, and 30 min incubations. A 0.1 μg aliquot of ASNS protein was incubated for the time indicated with substrate concentrations of 10 mM glutamine, 10 mM aspartate, and 1 mM ATP. (**B**) A protein concentration curve was assessed at 0.05, 0.1, 0.2, and 0.3 μg ASNS protein. The substrate concentrations were the same as for (A). (**C**) Measurement of glutamine K_m was achieved by varying the glutamine concentration to include 1, 3, 5, 10, or 20 mM. The results yielded an estimated K_m value for glutamine of 2.4 ± 0.04 mM. (**D**) Measurement of aspartate K_m was achieved by varying the aspartate concentration to include 0.25, 0.5, 1.0, 2.5, 5.0, and 10 mM. The calculated aspartate Km value was 0.53 ± 0.01 mM. All assays were performed in triplicate to assess variability within the assay and experiments were repeated with independently purified enzyme preparations to ensure reproducibility. Data are presented as means ± standard deviations. Where standard deviation bars are not shown, they are present within the symbol.

were stored at −80°C in a buffer containing 20% glycerol. Prior to freezing, each preparation was quantified by a Bradford assay and 2 μg was used for SDS–PAGE to confirm that the protein was without significant contaminants. The effect of temperature, −80°C versus 4°C, and days of storage on the enzymatic activity of WT ASNS protein was established (Fig. 4). These studies showed that the ASNS enzyme activity declined significantly after 3 days at 4°C, whereas protein stored at −80°C, and thawed only once, retained activity up to at least 10 days following purification. These results document that storage at −80°C and minimizing the time at 4°C prior to activity analysis will result in the most consistent results. It can also be inferred that optimizing the ASNS purification to minimize the time for affinity binding and elution at 4°C will also result in protein with the highest possible activity. Overall, the method described enables the purification of human WT ASNS and ASNSD variants and allows for comparative activity analysis of variants.

ASNS activity of known ASNSD variants

To illustrate the usefulness of the ASNS assay method, expression, purification, and enzymatic activity of three known ASNS protein variants were compared to WT. The variants were previously identified and partially characterized in primary fibroblasts from children afflicted with ASNSD [28, 29]. The specific substitutions were R49Q, G289A, and T337I (Fig. 5A). Using the human

ASNS crystal structure [33], computer modeling reveals that R49Q likely participates in the binding of glutamine within the N-terminal of ASNS [29], whereas the latter two are near the C-terminal region which catalyzes the formation of the aspartyl-AMP intermediate [28]. The computer modeling predicts that given the variants' proximity to the two active sites within ASNS, these substitutions may have a negative effect on enzymatic activity and this interpretation is supported by our reported observations of reduced proliferation in the absence of medium-supplied Asn of primary fibroblasts isolated from children harboring the substitutions [28, 29].

The stable overexpression of each variant in HEK 293T cells was confirmed by immunoblot analysis with a FLAG-specific monoclonal antibody (Fig. 5B). Ectopic expression of variant proteins in HEK 293T cells led to either modest increases or no difference in cell proliferation compared to regular HEK 293T cells. After purification the final yield was 16–20 μg pure protein from a starting amount of 7–10 mg cell lysate (Fig. 6A). This protein quantity is sufficient for 160–200 ASNS assay reactions. The high degree of purity for each protein preparation was confirmed by SDS–PAGE and Coomassie staining (Fig. 6B). The proteins were assayed for ASNS activity by the AMP detection method, with a negative control containing no ASNS protein. The results showed that compared to WT protein, the assayed variants have significantly decreased activity of 90% for R49Q, 36% for G289A, and
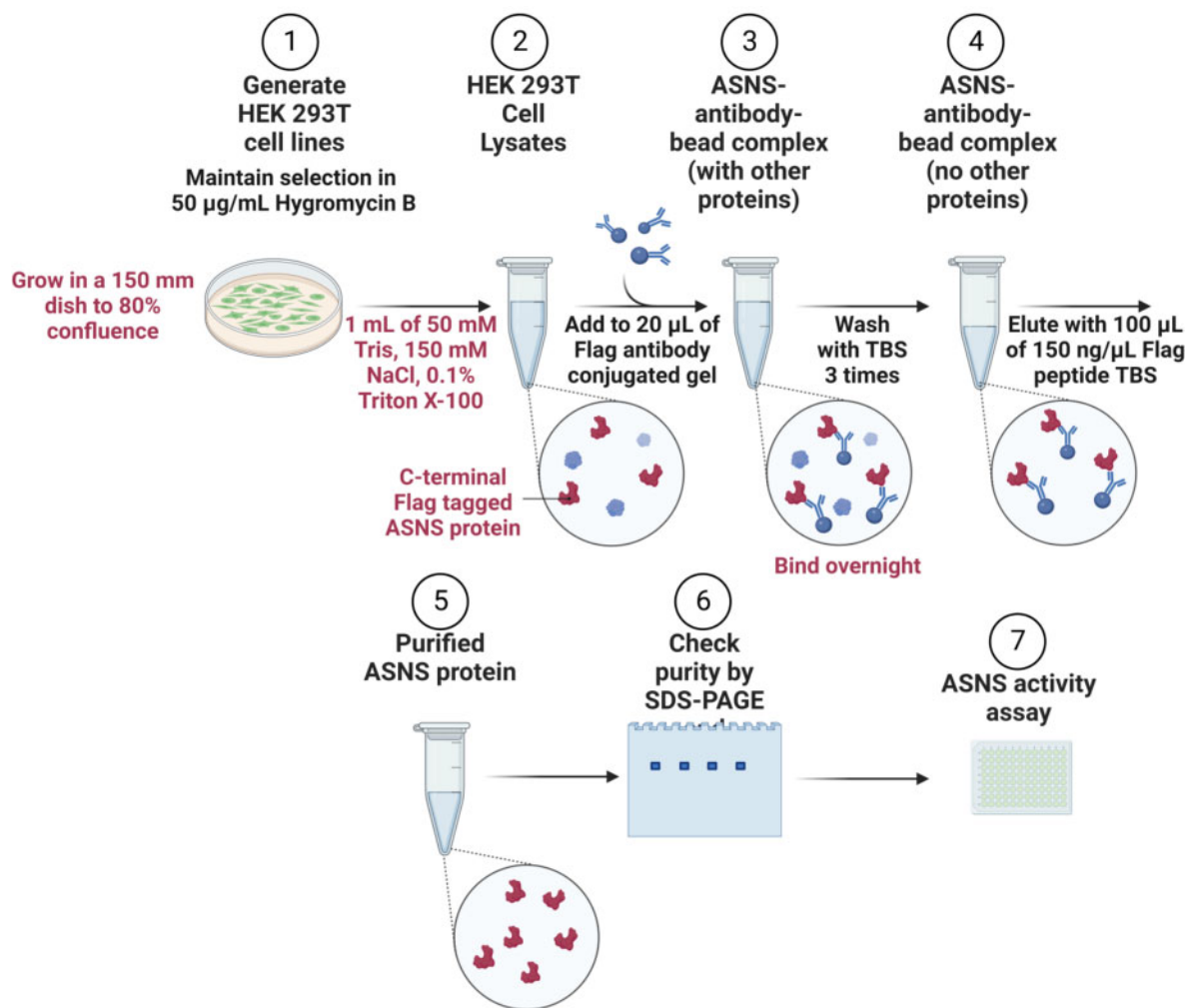
Figure 3. Flow diagram of the purification of C-terminal FLAG-tagged ASNS protein. Beginning with HEK 293T cells stably expressing WT or ASNS protein variants, the schematic shows the steps utilized to immunoprecipitate and purify C-terminal FLAG-tagged ASNS protein using gel-immobilized M2 anti-FLAG antibody. Protein purity was assessed by SDS–PAGE separation and staining with Coomassie Blue.
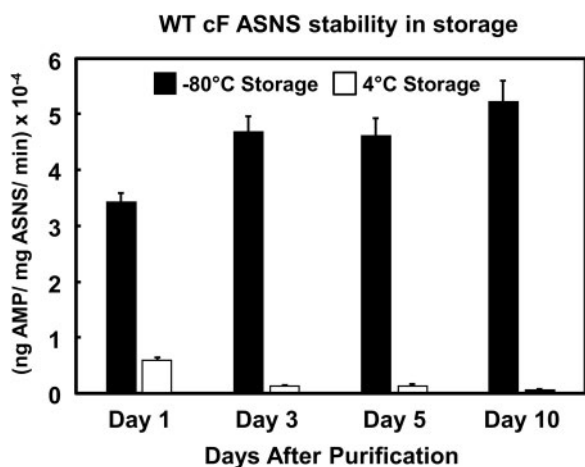

Figure 4. Stability of purified WT C-terminal FLAG-tagged ASNS. ASNS activity of purified WT ASNS-FLAG was measured after storage at either −80°C or 4°C for 10 days (N = 3 per group). Day 1 was defined as the day following purification and quantification.

96% for T337I (Fig. 6C). Collectively, the results provide novel insight into the previously reported ASNSD cases and validate the use of the newly developed ASNS activity assay.

Discussion

In this article, we describe a method to assay the enzymatic activity of ASNS by measurement of the AMP produced. In addition, a method for the purification of FLAG-tagged protein by immunoprecipitation is also presented. Both protocols can be performed in 3 days once the over-expressing cell lines are established. Previously reported ASNS activity methods used radioactive tracers, ninhydrin staining to detect amines, or HPLC [22–24]. Indeed, Matsumoto *et al.* used either ninhydrin staining or HPLC to measure Asn production of ASNSD-associated ASNS protein variants [22, 34]. While these methods are feasible, they are limited by their ease of use, sensitivity of detection, specificity, and reproducibility. In the approach described here, the measurement of ASNS-generated AMP product provides a simple protocol that
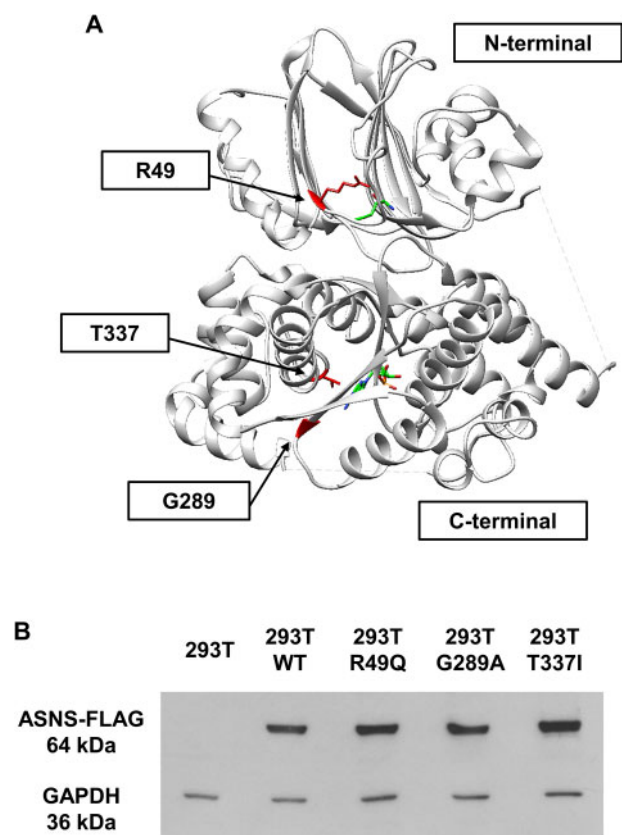
Figure 5. Modeling and over-expression of ASNS-FLAG variants associated with ASNSD. (**A**) Using the reported human ASNS crystal structure, the two domains, shown are the N-terminal domain that has glutamine binding and glutaminase activity and the C-terminal domain that catalyzes the synthesis of asparagine from aspartate and ATP. The locations of the R49Q, G289A, and T337I variants are shown in red. The C-terminal bound AMP product and the N-terminal bound glutamine substrate are shown with backbones in green, nitrogen atoms in blue, and oxygen atoms in red to illustrate the relative proximity of each variant to the substrate binding pockets. (**B**) Immunoblot analysis with FLAG antibody showing the relative levels of WT, R49Q, G289A, and T337I ASNS-FLAG variants for individual stably expressing HEK 293T cell lines.

Figure 6. Purification and activity analysis of ASNS WT and variants. (**A**) Summary of the starting protein content, concentrations after purification, and total yield of ASNS proteins prepared from HEK 293T cells stably expressing WT, R49Q, G289A, or T337I ASNS-FLAG. (**B**) SDS–PAGE of each purified ASNS-FLAG protein. Purified bands are seen at the expected 64 kDa for ASNS-FLAG protein. (**C**) Comparison of WT, R49Q, G289A, or T337I ASNS enzymatic activity. All assays were performed in triplicate within an experiment to evaluate variation and each experiment was repeated with an independent protein preparation to ensure reproducibility. Data are presented as means ± standard deviations and an asterisk denotes a $P \leq .01$ compared to the WT ASNS value.

eliminates the need for extensive chromatography or mass spectrometry equipment.

This approach is similar to that of Zhu *et al.*, who used a commercially available kit to measure the production of PPi by ASNS in their assessment of several ASNSD-associated ASNS protein variants [33]. Prior work has focused on measuring PPi production by measuring the UV/Vis absorbance of NADH or synthetically generated colorimetric compounds [32, 33, 35]. In principle, measuring PPi production with these methods also assumes that the stoichiometry of AMP formation is equivalent to Asn production since AMP and PPi are generated in the same step. Overall, absorbance-based methods are limited by higher backgrounds than bioluminescent assays and in particular, NADH-based assays are limited by the amount of stable NADH which can be degraded nonenzymatically [36].

While both absorbance and luminescence-based ASNS assays have their strengths and weaknesses, our experience with both indicates that measuring AMP production is more reproducible. Regarding ASNSD specifically, future studies involving over-expression and purification of ASNSD variants will not only permit t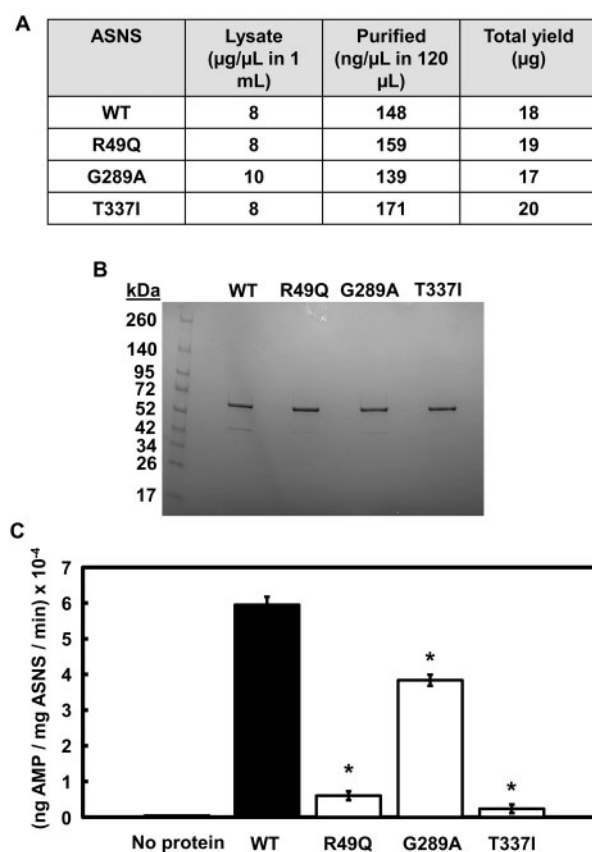he assessment of enzyme activity, but also complement structure determination by crystallography and direct protein stability studies. These combined approaches allow for a more complete structure–function analysis. We believe that this assay will serve as a valuable tool for researchers investigating diseases associated with changes in ASNS enzymatic activity.

Acknowledgements

Author contributions

Mario C. Chang (Conceptualization, Data curation, Formal analysis, Investigation, Methodology, Writing—original draft [equal]), Stephen J. Staklinski (Conceptualization, Data curation, Formal analysis, Investigation, Methodology, Writing—original draft [equal]), Matthew E. Merritt (Conceptualization, Investigation, Supervision, Writing—review and editing [equal]), and Michael S. Kilberg (Conceptualization, Funding acquisition, Investigation, Supervision, Writing—review and editing [equal]).

Funding

Data availability

The data presented in this manuscript are available through this journal article or will be readily available upon request.

References

1. Richards NGJ, Kilberg MS. Asparagine synthetase chemotherapy. *Annu Rev Biochem* 2006;**75**:629–54.
2. Broome JD. Studies on the mechanism of tumor inhibition by l-asparaginase. *J Exp Med* 1968;**127**:1055–72.
3. Kurtzberg J, Asselin BL. New Directions for Clinical Research. *Treatment of Acute Leukemias*. Totawa, NJ: Humana Press, 2003, 365–79.
4. Rizzari C. *Asparaginase Treatment. Treatment of Acute Leukemias*. Totawata, NJ: Humana Press, 2003, 381–91.
5. Aslanian AM, Kilberg MS. Multiple adaptive mechanisms affect asparagine synthetase substrate availability in asparaginase-resistant MOLT-4 human leukaemia cells. *Biochemical Journal* 2001;**358**:59–67.
6. Aslanian AM, Fletcher BS, Kilberg MS. Asparagine synthetase expression alone is sufficient to induce l-asparaginase resistance in MOLT-4 human leukaemia cells. *Biochem J* 2001;**357**:321–8.
7. Su N, Pan YX, Zhou M *et al.* Correlation between asparaginase sensitivity and asparagine synthetase protein content, but not mRNA, in acute lymphoblastic leukemia cell lines. *Pediatr Blood Cancer* 2008;**50**:274–9.
8. Pieters R, Hunger SP, Boos J *et al.* L-asparaginase treatment in acute lymphoblastic leukemia: a focus on Erwinia asparaginase. *Cancer* 2011;**117**:238–49.
9. Avramis VI. Asparaginases: biochemical pharmacology and modes of drug resistance. *Anticancer Res* 2012;**32**:2423–37.
10. Chiu M, Taurino G, Bianchi MG *et al.* Asparagine synthetase in cancer: beyond acute lymphoblastic leukemia. *Front Oncol* 2019;**9**:1480.
11. Krall AS, Xu S, Graeber TG *et al.* Asparagine promotes cancer cell proliferation through use as an amino acid exchange factor. *Nat Commun* 2016;**7**:11457.
12. Krall AS, Mullen PJ, Surjono F *et al.* Asparagine couples mitochondrial respiration to ATF4 activity and tumor growth. *Cell Metab* 2021;**33**:1013–26.e6.
13. Ruzzo EK, Capo-Chichi J-M, Ben-Zeev B *et al.* Deficiency of asparagine synthetase causes congenital microcephaly and a progressive form of encephalopathy. *Neuron* 2013;**80**:429–41.
14. Lomelino CL, Andring JT, McKenna R *et al.* Asparagine synthetase: function, structure, and role in disease. *J Biol Chem* 2017;**292**:19952–8.
15. Sprute R, Ardicli D, Oguz KK *et al.* Clinical outcomes of two patients with a novel pathogenic variant in ASNS: response to asparagine supplementation and review of the literature. *Hum Genome Var* 2019;**6**:24.
16. Liu L, Wang J, Li H *et al.* An intractable epilepsy phenotype of ASNS novel mutation in two patients with asparagine synthetase deficiency. *Clin Chim Acta* 2022;**531**:331–6.
17. Hawkins RA, O'Kane RL, Simpson IA *et al.* Structure of the blood-brain barrier and its role in the transport of amino acids. *J Nutr* 2006;**136**:218S–26S.
18. Alfadhel M, Alrifai MT, Trujillano D *et al.* Asparagine synthetase deficiency: new inborn errors of metabolism. In: Zschocke J, Baumgartner M, Morava E *et al.* (eds.), *JIMD Reports*, Vol. **22.** Berlin, Heidelberg, Germany: Springer Berlin Heidelberg, 2015, 11–6.
19. Seidahmed MZ, Salih MA, Abdulbasit OB *et al.* Hyperekplexia, microcephaly and simplified gyral pattern caused by novel ASNS mutations, case report. *BMC Neurol* 2016;**16**:105.
20. Yamamoto T, Endo W, Ohnishi H *et al.* The first report of Japanese patients with asparagine synthetase deficiency. *Brain Dev* 2017;**39**:236–42.
21. Gupta N, Tewari VV, Kumar M *et al.* Asparagine synthetase deficiency-report of a novel mutation and review of literature. *Metab Brain Dis* 2017;**32**:1889–900.
22. Moore S, Stein WH. Photometric ninhydrin method for use in the chromatography of amino acids. *J Biol Chem* 1948;**176**:367–88.
23. Unnithan S, Moraga DA, Schuster SM. A high-performance liquid chromatography assay for asparagine synthetase. *Anal Biochem* 1984;**136**:195–201.
24. Cooney DA, Homan E, Cameron T *et al.* The measurement of 4- (14 C)-L-asparagine in body fluids and tissues: methodology and application. *J Lab Clin Med* 1973;**81**:455–66.
25. Chan WK, Tan L, Harutyunyan K *et al.* The glutaminase activity of L-asparaginase mediates suppression of ASNS upregulation. *Blood* 2018;**132**:3959.
26. Staklinski SJ, Chang MC, Yu F *et al.* Cellular and molecular characterization of two novel asparagine synthetase gene mutations linked to asparagine synthetase deficiency. *J Biol Chem* 2022; **298**:102385.
27. Staklinski SJ, Chang MC, Ahrens-Nicklas RC *et al.* Characterizing asparagine synthetase deficiency variants in lymphoblastoid cell lines. *JIMD Rep* 2023;**64**:167.
28. Palmer EE, Hayner J, Sachdev R *et al.* Asparagine synthetase deficiency causes reduced proliferation of cells under conditions of limited asparagine. *Mol Genet Metab* 2015;**116**:178–86.
29. Sacharow SJ, Dudenhausen EE, Lomelino CL *et al.* Characterization of a novel variant in siblings with asparagine synthetase deficiency. *Mol Genet Metab* 2018;**123**:317–325.
30. Staklinski SJ, Snanoudj S, Guerrot AM *et al.* Analysis of enzyme activity and cellular function for the N80S and S480F asparagine synthetase variants expressed in a child with asparagine synthetase deficiency. *Int J Mol Sci* 2022;**24**:559.
31. Larsen TM, Boehlein SK, Schuster SM *et al.* Three-dimensional structure of *Escherichia coli* asparagine synthetase B: a short journey from substrate to product. *Biochemistry* 1999; **38**:16146–57.
32. Ciustea M, Gutierrez JA, Abbatiello SE *et al.* Efficient expression, purification, and characterization of C-terminally tagged, recombinant human asparagine synthetase. *Arch Biochem Biophys* 2005;**440**:18–27.
33. Zhu W, Radadiya A, Bisson C *et al.* High-resolution crystal structure of human asparagine synthetase enables analysis of inhibitor binding and selectivity. *Commun Biol* 2019;**2**:345.
34. Matsumoto H, Kawashima N, Yamamoto T *et al.* In vitro functional analysis of four variants of human asparagine synthetase. *J Inherit Metab Dis* 2021;**44**:1226–34.
35. Upson RH, Haugland RP, Malekzadeh MN *et al.* A spectrophotometric method to measure enzymatic activity in reactions that generate inorganic pyrophosphate. *Anal Biochem* 1996;**243**:41–5.
36. Rover L, Fernandes JCB, Neto GDO *et al.* Study of NADH stability using ultraviolet–visible spectrophotometric analysis and factorial design. *Anal Biochem* 1998;**260**:50–5.